Journal of Advanced Research in Applied Sciences and Engineering Technology

Journal homepage:
https://semarakilmu.com.my/journals/index.php/applied_sciences_eng_tech/index
ISSN: 2462-1943

An MPPT Controller with a Modified Four-Leg Interleaved DC/DC Boost Converter for Fuel Cell Applications

Arigela Satya Veerendra[1,*], Kumaran Kadirgama[2], Sivayazi Kappagantula[3], Subbarao Mopidevi[4], Norazlianie Sazali[5]

[1] Department of Electrical and Electronics Engineering, Manipal Institute of Technology, Manipal Academy of Higher Education, Manipal, Karnataka 576104, India
[2] Faculty of Mechanical and Automotive Engineering Technology, Universiti Malaysia Pahang, 26600 Pekan, Pahang, Malaysia
[3] Department of Mechatronics, Manipal Institute of Technology, Manipal Academy of Higher Education (MAHE), Manipal, Karnataka 576104, India
[4] Vignan's Foundation for Science, Technology & Research, Guntur, Andhra Pradesh 522213, India
[5] Faculty of Manufacturing and Mechatronic Engineering Technology, University Malaysia Pahang, 26600 Pekan, Pahang, Malaysia

ABSTRACT

A fuel cell system can produce electricity and water more efficiently while emitting near-zero emissions. Internal constraints and operating parameters such as hydrogen, temperature, humidity levels, and oxygen gas partial pressures trigger a nonlinear power characteristic in a typical fuel cell stack, resulting in reduced overall system efficiency. Consequently, it's critical to get the most power out of the fuel cell stack while minimizing fuel use. This study examines and proposes a radial basis function network (RBFN) based maximum power point tracking technique (MPPT) for a 6-kW proton exchange membrane fuel cell (PEMFC) system. The proposed MPPT algorithm modulates the duty cycle of the modified four-leg interleaved DC/DC boost converter (MFLIBC) to extricate the maximum power from the fuel cell system. To validate the execution of the proposed controller, the outcome is related to the various MPPT control strategies such as PID & Mamdani fuzzy inference systems. Finally, it was observed that the proposed RBFN controller has achieved an enhanced efficiency of 83.2 % relative to the PID and fuzzy logic controllers of 75.5 % and 77.4 % respectively. The efficiency of the proposed configuration is analysed using the MATLAB/Simulink platform.

Keywords:

Interleaved boost converter; Fuzzy controller; MPPT controller; Fuel cell system; Neural network

1. Introduction

The global environmental damage caused by the use of fossil fuels has raised the need for alternative power sources. Owing to their impressive reduction in greenhouse gas emissions, the transition to renewable energy sources has gotten more attention in recent years in the transportation sector. Fuel cell (FC) systems are viewed as a possible alternative renewable energy source to meet rising energy demands due to their zero emissions [1-4]. Among all types of fuel

* *Corresponding author.*
E-mail address: veerendra.babu@manipal.edu

https://doi.org/10.37934/araset.53.1.219236

cells, the Proton exchange membrane fuel cell (PEMFC) is the most suitable type of fuel cell for automotive applications and even residential combined heat and power systems owing to its lightweight, low cost, and flexibility in input fuel. However, the output V-I characteristics of the fuel cell system are nonlinear, and dependent on internal constraints like cell temperature and membrane water content, resulting in reduced overall system efficiency. Therefore, it is essential to use a maximum power point tracking (MPPT) controller to always extract the highest amount of power, regardless of fuel cell parameter variations [5-7].

An extensive review of the various MPPT techniques has been discussed in the previous literature [8-10]. Among all MPPT algorithms, the perturb & observe (P&O) method is the most popular one. The P&O algorithm is the simplest and most classical form of sensorless MPPT control technique. However, this method fails to track the maximum power owing to the rapid change in the fuel cell operating point [11,12]. Later, to overcome the above limitation an incremental conductance method is presented in [13]. Nevertheless, the proposed method generates oscillations at peak power points which will reduce the efficiency of the fuel cell system. Benyahia *et al.,* [14] discussed a modified conventional MPPT controller for an interleaved boost converter utilized in fuel cell electric vehicle applications. However, the controller generates the oscillations because of the usage of the conventional P&O method. Besides, a neural network-based MPPT algorithm for fuel cell application is discussed in [15]. This method is used to extricate the maximum power from the fuel cell at various operating temperatures. However, the efficiency analysis is missing in this article. Furthermore, an improved fuzzy logic controller-based MPPT algorithm is used for the PEMFC system is discussed in [16]. This study validated the efficiency of the proposed method with an incremental conductance method. However, the main limitation of the MPPT controller is the high settling time to reach the steady-state.

Mokhtar Aly *et al.,* [17] proposed an optimized fuzzy logic MPPT algorithm for extracting the utmost power from the fuel cell system. Subsequently, the grey wolf optimizer (GWO) [18], the particle swarm optimization (PSO) [19], and the Antlion optimizer (ALO) [20] have been designed to tune the proportional-integral-derivative (PID) controllers to monitor the PEMFC system's maximum power output. However, the complexity of designing the controller is the major limitation of the above algorithms. Later, Fathy *et al.,* [21] proposed a salp swarm algorithm for extricating the utmost power from the fuel cell system. Nevertheless, the study fails to identify the efficiency and settling time of the PEMFC system. Furthermore, a novel hybrid MPPT controller based on fuzzy logic and bond graph methods has been discussed in [22]. This study evaluates the efficiency of the proposed controllers with two more controllers such as fuzzy logic and PSO algorithms. However, the main limitation of the work is the high settling time to reach the study state. Besides, Gugulothu *et al.,* [23] developed a Jaya algorithm-based MPPT controller to monitor the maximum power from the PEMFC system. In this work, the proposed algorithm achieves an efficiency of 81.6 % and a settling time of 0.12 s relative to the conventional techniques. However, high steady-state time and reduced efficiency are the major limitations of the study.

In this article, an RBFN-P&O-based MPPT controller is implemented for FC applications in the MATLAB/Simulink software. The proposed MPPT algorithm modulates the duty cycle of the modified FLIBC to extract the maximum power from the fuel cell system. Finally, to validate the performance of the proposed configuration, the result is compared with the different MPPT control strategies namely PID-P&O & Mamdani Fuzzy Inference-P&O Systems. This assesses the execution of various MPPT controllers in terms of voltage, current, power, settling time, and efficiency.

2. Methodology

2.1 Modified Four-Leg Interleaved Boost Converter

Figure 1(a) shows the conventional four-leg interleaved boost converter (FLIBC) topology of the DC/DC converter that can be used in fuel cell-based hybrid electric vehicles [24]. The fuel cell input voltage is Vfc; S1, S2, S3, and S4 are the main switches; L1, L2, L3, and L4 are the inductors; D1, D2, D3, and D4 are the diodes; C is the capacitor; and the resistor is referred to as the load.

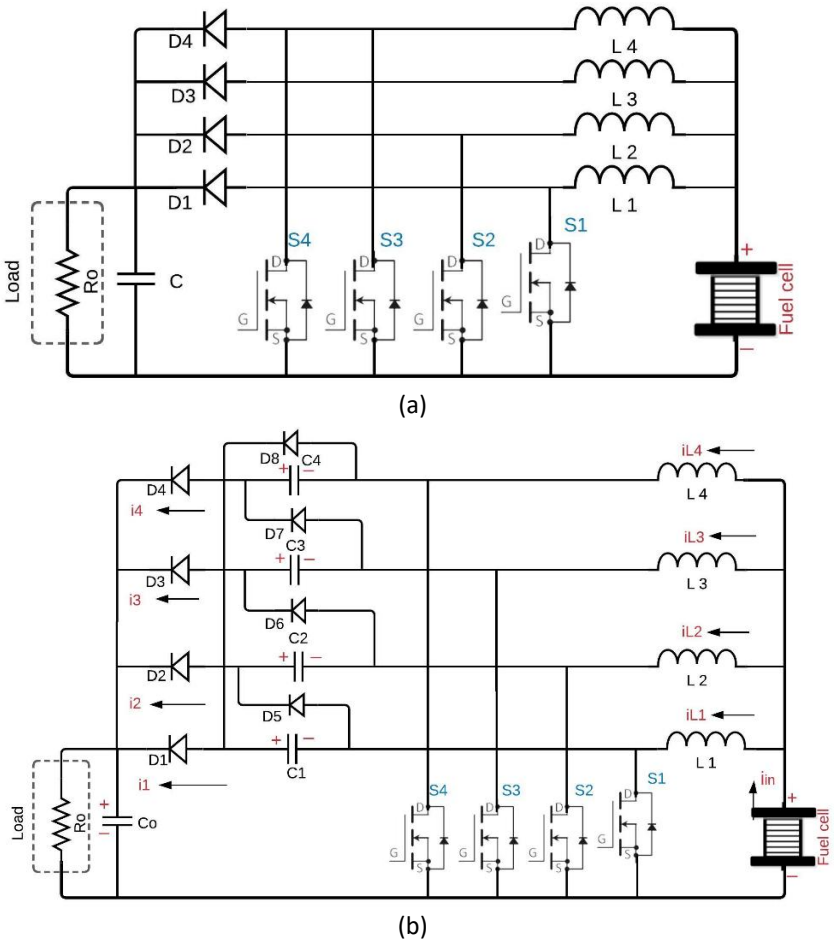

Fig. 1. (a) Conventional FLIBC topology (b) MFLIBC topology

The capacitor voltages can be given as follows Eq. (1);

$$V_{C1} = V_{C2} = V_{C3} = V_{C4} = \frac{V_{in}}{1-D} \tag{1}$$

The values for the capacitance and inductance are calculated as follows Eq. (2) and Eq. (3);

$$C_0 = \frac{V_0\, D}{\Delta V_0 . R_L . f} \tag{2}$$

$$C_0 = \frac{V_0\, D}{\Delta V_0 . R_L . f} \tag{3}$$

$$L = \frac{V_{in} . D}{f . \Delta I_L}$$

The output voltage can be given as follows Eq. (4);

$$V_o = \frac{2V_{in}}{1-D} \tag{4}$$

The converter used in this article is a traditional FLIBC coupled with another interleaved converter with a voltage multiplier, as shown in Figure 1(a), and is referred to as a modified four-leg interleaved boost converter (MFLIBC). The modes of operation are discussed in [25]. Assume all the devices are ideal, the capacitors C1, C2, C3, and C4 are large enough while all the capacitors and the inductors are referred to as C and L respectively during the operation. The four legs are phase-shifted by $T_s/4$. The specifications of the IBC topologies are given in Table 1.

Table 1
Specifications of fuel cell and interleaved boost converter

Parameters	Ratings
Input voltage (PEMFC)	6kW-45 V
Nominal operating point [I_{nom}(A), V_{nom} (V)]	[133.3 45]
Nominal stack efficiency	55 %
Number of cells	65
Maximum operating point [I_{end} (A), V_{end}(V)]	[225 37]
Operating temperature	338K
Inductor (L)	300 μH
Capacitor (C)	100 μF
Resistor	100 Ω

The main use of the MPPT algorithm in fuel cell systems is to operate the structure with peak efficiency. The power converter is controlled by the MPPT algorithm, thereby making it work at its maximum PowerPoint. Among all MPPT algorithms, the perturb & observe (P&O) method is the most popular one owing to its easy implementation [14]. However, this method fails to track the maximum power owing to the rapid change in the fuel cell operating point. To overcome the above limitation in this study the following controllers have been combined to control the duty cycle of the MFLIBC. Figure 2 depicts the flow chart of the P&O algorithm.

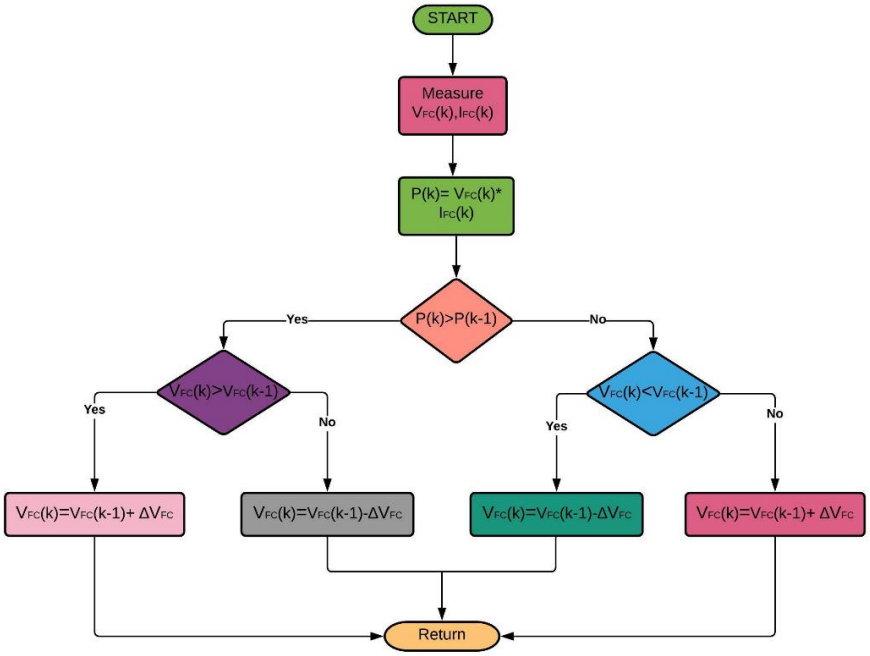

Fig. 2. P&O MPPT algorithm

2.2 PID Controller

A PID controller is the most widely utilized controller in the industry. It is a conventional controller that regulates past, current, and future values over time. It reduces both the steady-state error and transient response.

It is a combination of three different controllers connected in parallel which are proportional variables denoted as P, an integral variable denoted as I, and a derivative variable denoted as D. The rise time is improved by the proportional variable, the overshoot is improved by the integral variable, and the steady-state error is eliminated by the derivative variable. These three variable gains have been fine-tuned to achieve the desired performance while maintaining a fast dynamic response. It is a feedback control mechanism that entails an error signal to be stimulated. The equation for the system's error is formulated as follows Eq. (5);

$$e(t) = V_{ref} - V_{out} \tag{5}$$

The equation for the proportional controller's output response is formulated as follows Eq. (6);

$$P_o = K_p e(t) \tag{6}$$

The equation for the derivative controller's output response is formulated as follows Eq. (7);

$$D_o = K_d \frac{de(t)}{dt} \tag{7}$$

The equation for the PID controller's output response is formulated as follows Eq. (8);

$$y(t) = K_p e(t) + K_i \int e(t)\, dt + K_d \frac{de(t)}{dt} \tag{8}$$

Where K_p is the proportional gain, K_i is the integral gain and K_d is the derivative gain.

2.2.1 Fuzzy controller

Fuzzy logic is based on human decision-making and can produce good efficiency or reasonable performance without understanding a specific mathematical model with uncertain inputs. From Figure 3 it can be observed that there are four major and essential steps in implementing any fuzzy system such as; Fuzzification, rule base, inference engine, and defuzzification. The fuzzy toolbox of MATLAB software has been used to build a fuzzy structure and construct membership functions and rule bases. It attempts to keep the difference between the actual and reference values as small as possible.

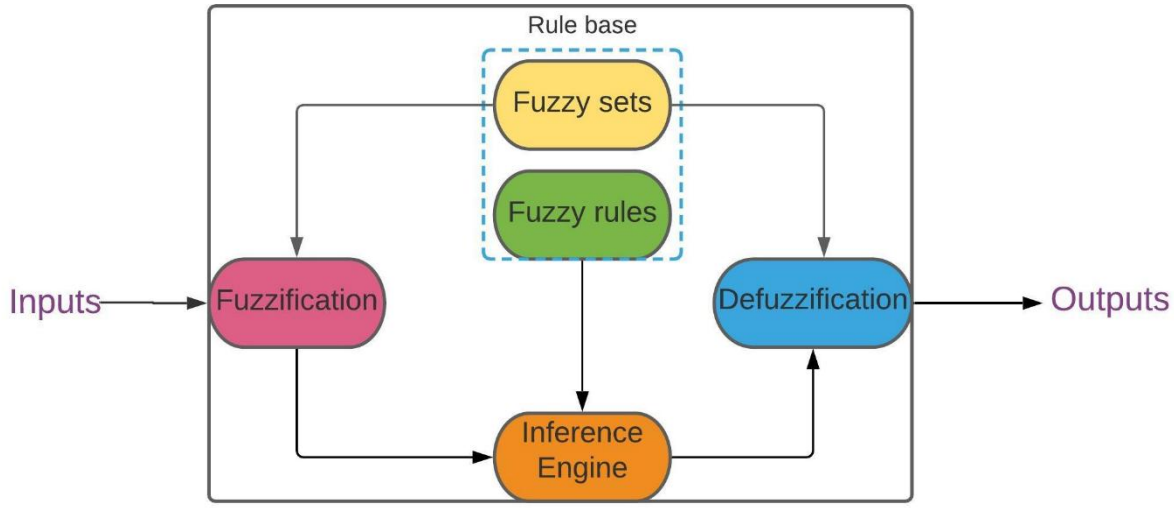

Fig. 3. Basic structure of FLC

In general, two inputs are defined as inputs to the controller in terms of memberships, namely error and adjustment in error, and the controller's yield is also expressed in terms of membership functions. Table 2 lists the fuzzy inference rules.

Table 2
Fuzzy inference rules

E CE	NB	NM	NS	ZE	PS	PM	PB
NB	NB	NB	NB	NB	NM	NS	ZE
NM	NB	NB	NB	NM	NS	ZE	PS
NS	NB	NB	NM	NS	ZE	PS	PM
ZE	NB	NM	NS	ZE	PS	PM	PB
PS	NM	NS	ZE	PS	PM	PB	PB
PM	NS	ZE	PS	PM	PB	PB	PB
PB	ZE	PS	PM	PB	PB	PB	PB

The fuzzy controller receives two inputs: the error between the integrated system's PowerPoint voltage and the actual voltage, and the change in error. These are fed into the fuzzifier as input to transform crisp variables. Then the two inputs of the transformed fuzzy membership functions

were then subjected to a seven-variable analysis: negative big (NB), negative medium (NM), negative small (NS), zero (ZE), positive big (PB), positive medium (PM), positive small (PS).

$$IF\ R\ THEN\ \mu(x) \tag{9}$$

The fuzzy rules and the AND operation can be expressed as follows Eq. (10);

$$\mu A \cap B(x) = min[\mu A(x), \mu B(x)] \tag{10}$$

The equation for the system's error is as follows Eq. (11);

$$e(t) = V_{ref} - V_{out} \tag{11}$$

The equation for the system's change in error is as follows Eq. (12);

$$\frac{de(t)}{dt} = \frac{d[V_{ref} - V_{out}]}{dt} \tag{12}$$

The membership value can be calculated using the following Eq. (13)

$$\mu(x) = \{0; x < a$$
$$\mu(x) = \{1; x > a \tag{13}$$

The equation for the value of the Guass bell function is as follows Eq. (14);

$$\mu(x) = e^{-\frac{(x-C_f)}{W}} \tag{14}$$

where W is the parameter ; C_f is the nucleus of fuzzy set

Partitions of the fuzzy subsets and the shape of the membership function are displayed in Figure 4.

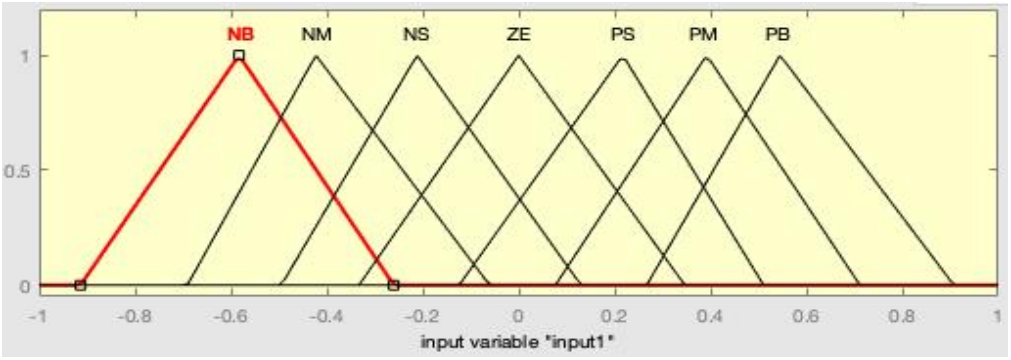

(a)

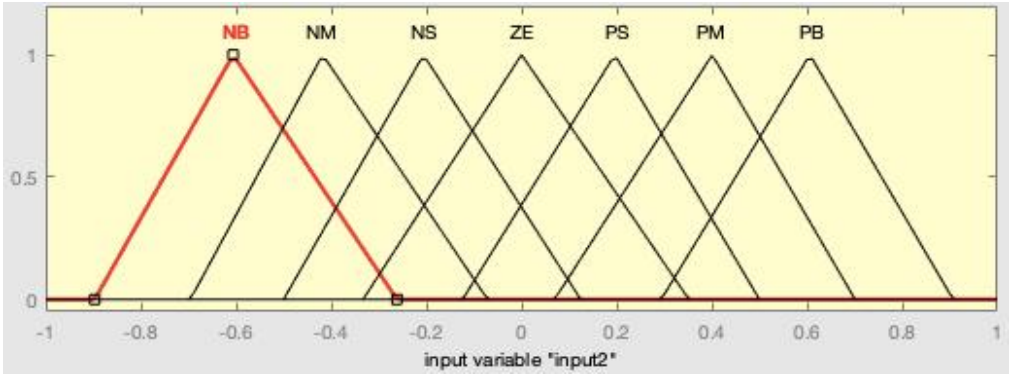

(b)

Fig. 4. Input membership functions (a) Error (b) Change of Error

Furthermore, Figure 5 represents the output variable. The triangular shapes of this arrangement membership function imply that there is only one dominant fuzzy subset for any given input. The fuzzy rule base is formulated into 49 rules using the tabulated in Table 2.

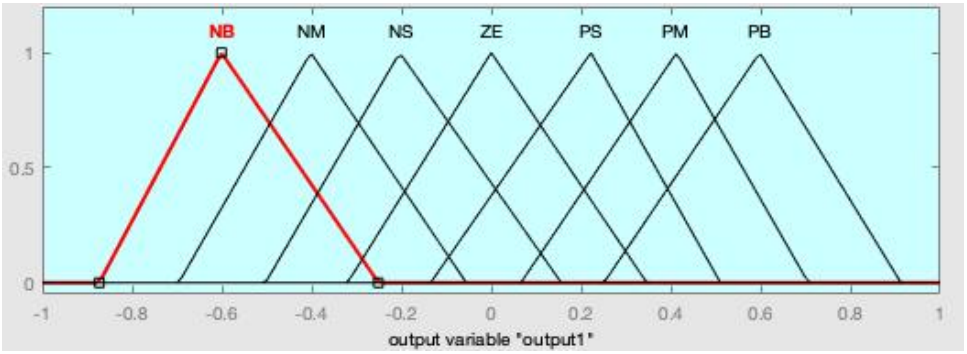

Fig. 5. Output variable

Following the configuration of the membership functions, the fuzzy controller's rules must be written. The rules are chosen based on knowledge and experience.

The fuzzy output membership function was then defuzzified using the centroid form of the defuzzification method to produce a crisp value. Figure 6 depicts the surface of the fuzzy controller utilizing the previous rules. The surface displays the relationship between the inputs and output at any point in the intervals [-1,1]. The crisp value from centroid defuzzification can be calculated by the following Eq. (15).

$$X = \frac{\int \mu(x) x dx}{\mu(x) dx} \tag{15}$$

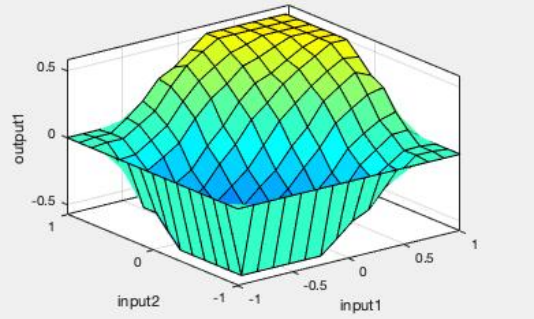

Fig. 6. Surface of fuzzy controller

2.2.2 Artificial neural network

Artificial neural networks (ANNs) are a type of artificial intelligence technique that allows for an approximate non-linear relationship between a complex system's inputs and outputs without needing an explicit mathematical model. They have the ability to learn from their mistakes, improve their results, and adapt to changes in the world. ANN is built on the foundations of the human nervous system. To achieve a quick, steady-state response, the human nervous system's analogous components have all been designed to work together to simulate a human neural system.

Here in this study, a RBFN type is used for the ANN controller. It is made up of inputs that are weighted, the sum of which is then passed through the activation function to obtain the controller-supplied amount, which is then sent to the device. The process is repeated until the error is zero. The weighted sum of the neural network can be expressed as follows Eq. (16).

$$NET = \sum_{i=1}^{n} W_i X_i \tag{16}$$

The net sum, also known as the weighted sum, can be expanded as follows Eq. (17);

$$NET = W_1X_1 + W_2X_2 + W_3X_3 + W_4X_4 + \cdots\cdots\cdots\cdots + W_nX_n \tag{17}$$

The hidden layer's net sum is guided to the tan sigmoid activation feature, which generates hidden layer output. This output from the hidden layer travels via the weight and into the output layer, producing NET once more. The RBFN structure is shown in Figure 7.

$$y = f(NET) \tag{18}$$

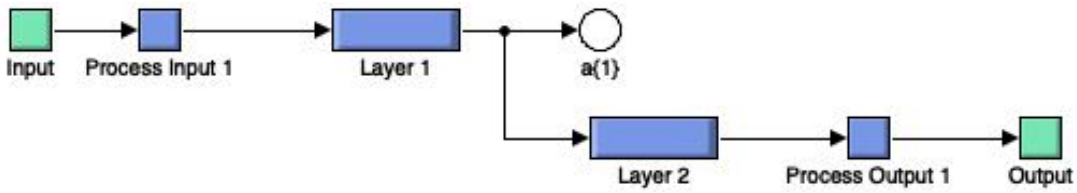

Fig. 7. Radial basis function network structure

The linear activation function passes the NET value at the output layer, which can be expressed as Eq. (19) and Eq. (20)

$$NET_y = WY \tag{19}$$

$$Z = f(NET_y) = f(wy) = wyNET = \sum_{i=1}^{n} W_i X_i \quad (20)$$

In addition, the tracking efficiency is the most precious parameter to assess the accuracy of the MPPT controller. Hence, the efficiency can be determined as follows Eq. (21).

$$\eta(\%) = \frac{P_{MPPT}}{P_{MPP}} \times 100 \quad (21)$$

where, P_{MPPT} is the output power and the P_{MPP} is the maximum power of the fuel cell stack.

The block diagram of the proposed controller for the PEMFC system is shown in the following Figure 8. The above techniques are used to generate gate pulses while maintaining maximum voltage, current, and power values. The PEMFC system's voltage and current data are first provided as inputs to the P&O MPPT controller. Then, with a given number of disturbances, changes in power and voltage will be planned, and maximum voltage will be calculated using these values. Later, the obtained value is relative to the actual value of the fuel cell system. Finally, the response of the comparator is evaluated by the various controllers, which will generate gate pulses for the modified four-leg interleaved boost converter using the pulse width modulation technique.

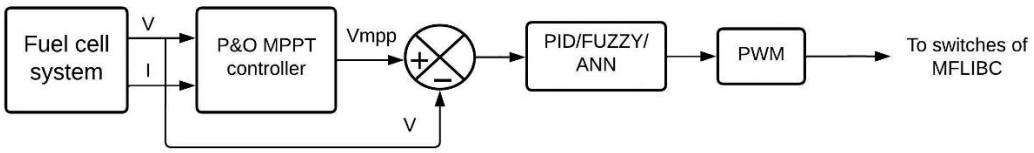

Fig. 8. Block diagram of proposed controller

3. Results

The proposed system was simulated in the MATLAB/Simulink environment. The simulation results were used to assess the system's accuracy. Initially, to validate the results of the proposed controllers with M-FLIBC, conventional FLIBC-based operations were done and corresponding outputs were displayed in the respective sections as follows for comparison. The specifications of the proposed topology with an FC as well as converter are shown in Table 1 respectively. After designing the entire system, the PID-based P&O MPPT, Fuzzy-based P&O MPPT, and RBFN-based P&O MPPT controllers have been used to evaluate the performance of the system.

3.1 PID-Based P&O MPPT controller

The FC is directly given to the M-FLIBC and then the output responses have been analysed across the load. Here the gate signals are fed to the power electronic switches with the help of PID based P&O MPPT controller. The FC input voltage, current, and power waveforms have been depicted in Figure 9.

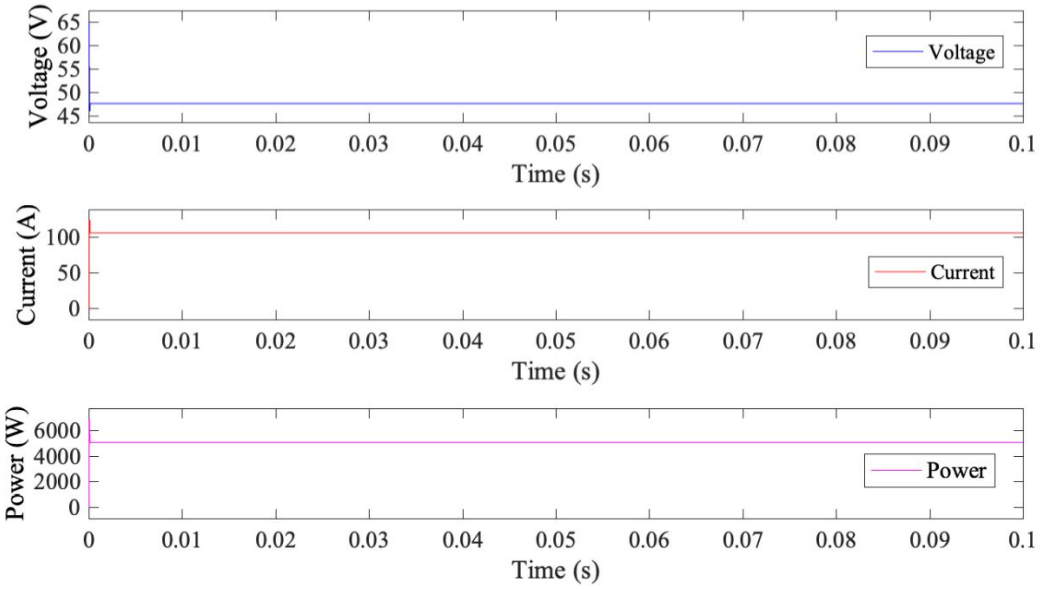

Fig. 9. Responses of the FC system

The corresponding output waveforms from the modified four-leg interleaved boost converter and the conventional topology are presented in Figure 10 respectively.

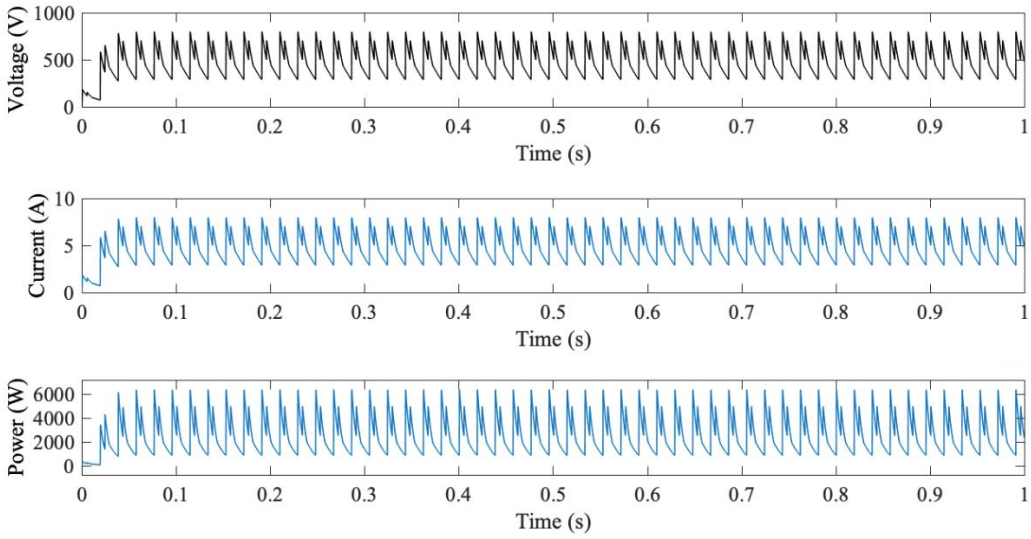

(a)

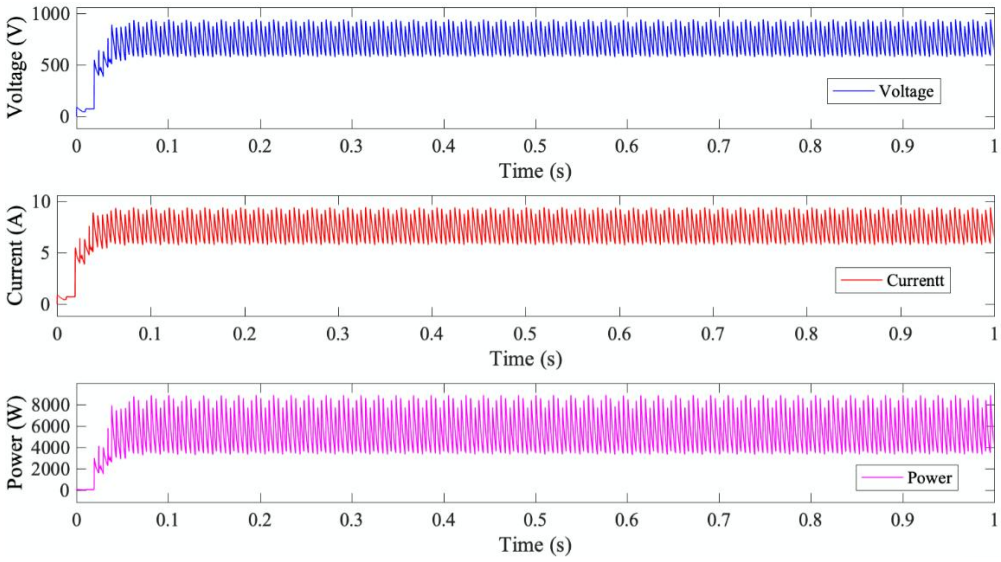

(b)

Fig. 10. (a) FLIBC responses across the load using PID – P&O MPPT controller, (b) M-FLIBC responses across the load using PID – P&O MPPT controller

The output responses across the FC system were given as the input to the converter topologies. Here it is noted that while using the conventional FLIBC the input parameters which can be obtained across the FC systems such as voltage, current, and power are obtained as 46.3 V, 102.9 A, and 4356 W respectively. The corresponding output parameters across the load are achieved to be 436.3 V,4.36 A, and 2954 W respectively.

Furthermore, the conventional FLIBC is replaced with the M-FLIBC then the input parameters such as voltage, current, and power are observed as 47.53 V, 105.6 A, and 5020 W respectively. The output responses of the system at the load side are 623.5 V, 6.235 A, and 3887 W respectively. The settling time of the responses from the converter was at 0.06s each whereas for the conventional converter it is noted as 0.071s respectively.

3.2 Fuzzy Based P&O MPPT Controller

The proposed system was modelled and simulated with fuzzy-based P&OMPPT controller and the following results were obtained. The FC system responses have been given as input to the proposed topology and the corresponding outputs from the converter are analysed. It is studied that the proposed controllers with conventional FLIBC have the output voltage of 458.7 V, the output current of 4.58 A, and the maximum output power extracted from the converter of 3126 W respectively is depicted in Figure 11(a).

Whereas with the M-FLIBC the output voltage, current, and power are generated as 615.9 V, 6.159 A, and 3794 W respectively as shown in Figure 11(b). During the operations of both the converters with the fuzzy -based P&O MPPT controller, the settling time of the responses was observed at the time of 0.068s and 0.051s each.

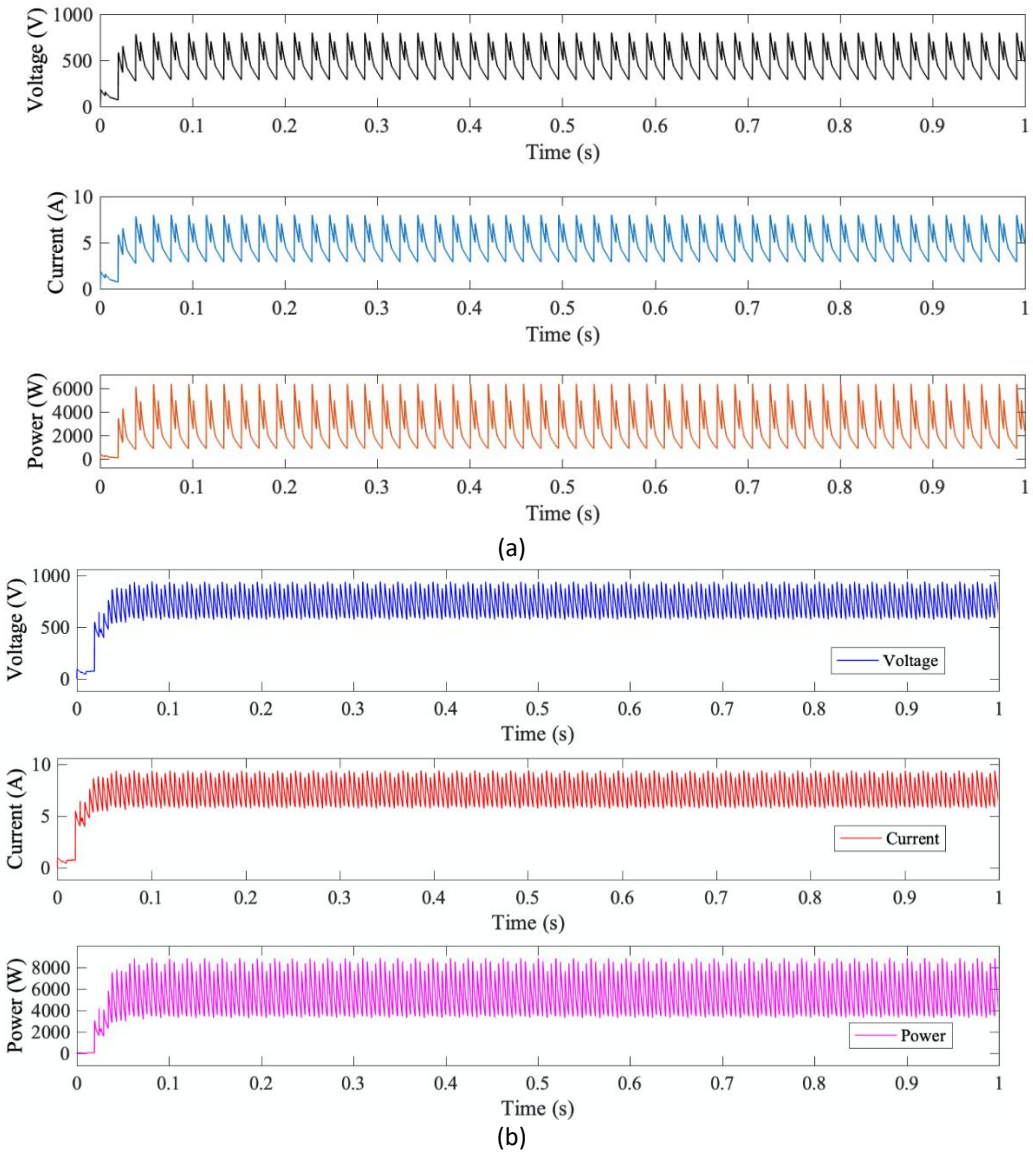

Fig. 11. (a) FLIBC responses across the load using Fuzzy-P&O MPPT controller, (b) M-FLIBC responses across the load using Fuzzy-P&O MPPT controller

3.3 RBFN-P&O MPPT Controller

The proposed system was modelled and simulated with an RBFN-based P&O MPPT controller and the following results were obtained. Here it is noted that while using the conventional FLIBC the input parameters that can be obtained across the FC system such as voltage, current, and power are obtained as 46.3 V, 102.9 A, and 4356 W respectively. The corresponding output parameters across the load are achieved to be 484.6 V, 4.84 A, and 3489 W respectively are displayed in Figure 12(a).

Similarly, when the proposed controllers have been operated with M-FIBC having the input voltage of 47.53 V, current of 105.6 A, and power of 5020 W then the generated responses at the terminals of the load in terms of voltage, current, and power are 646.3 V and 6.463 A, and the power of 4177 W respectively as shown in Figure 12(b). The settling time of the responses from the converter was at 0.046s each whereas for the conventional converter, it is noted as 0.062s respectively.

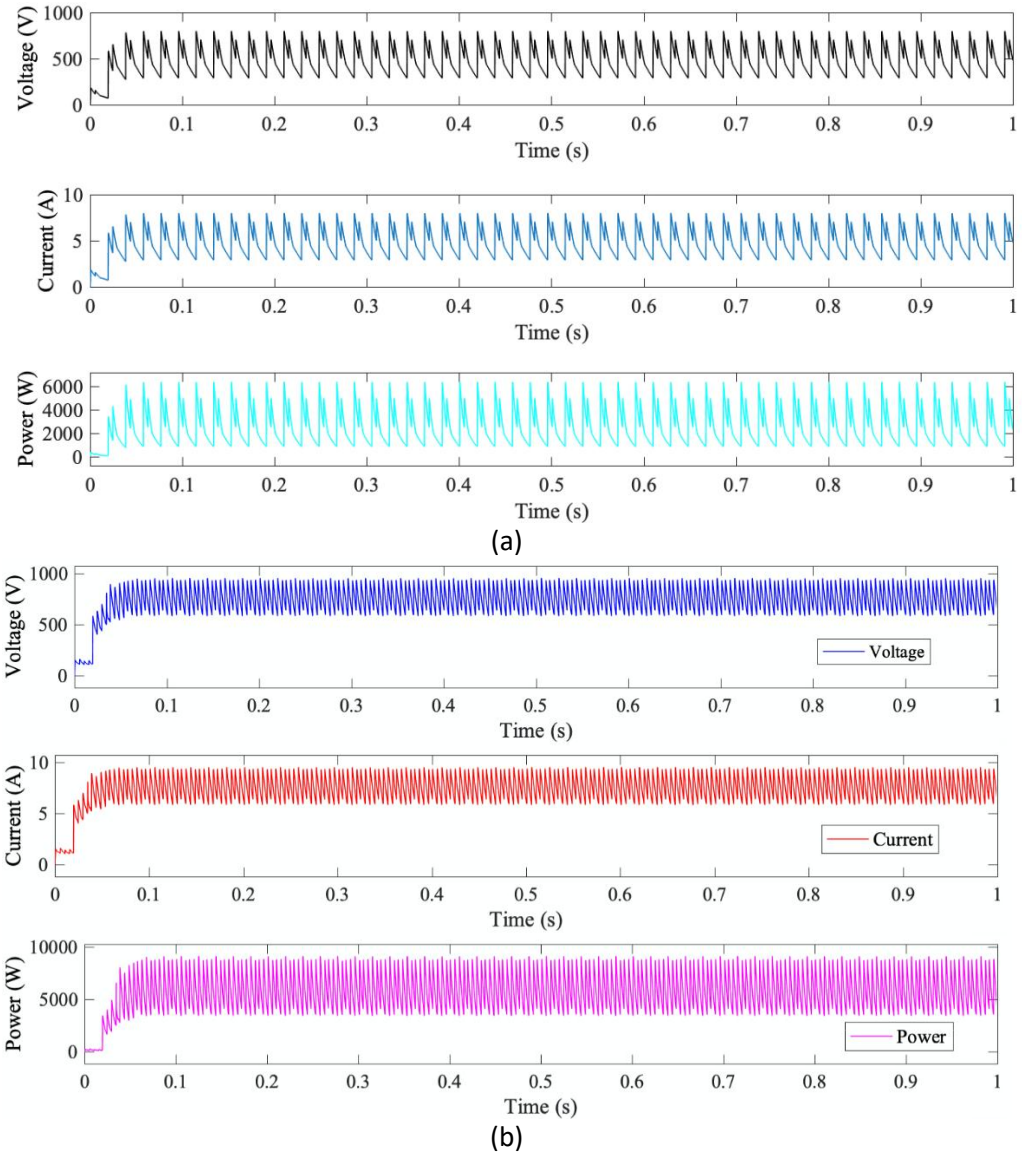

Fig. 12. (a) FLIBC responses across the load using RBFN-P&O MPPT controller, (b) M-FLIBC responses across the load using RBFN-P&O MPPT controller

The comparison of the controllers such as PID based P&O MPPT, Fuzzy based P&O MPPT and the RBFN based P&O MPPT in terms of voltage, current, power as well as efficiency, were discussed in Table 3 and corresponding figures have been displayed in Figure 13. It was observed that the RBFN-based P&O MPPT controller shows better performance compared to the other two controllers. Moreover, the tracking efficiency of the system is observed as 83.2 % relative to the PID-based P&O MPPT and fuzzy-based P&O MPPT controllers. As well as the M-FLIBC with the proposed controllers has been given better responses compared with the conventional FLIBC topology.

Table 3
Comparison of the three controllers

Parameters	PID-P&O MPPT		Fuzzy-P&O MPPT		RBFN-P&O MPPT	
	Conventional topology	Proposed topology	Conventional topology	Proposed topology	Conventional topology	Proposed topology
DC voltage (V)	436.3	615.9	458.7	623.5	484.6	646.3
DC current (A)	4.36	6.15	4.58	6.23	4.84	6.46
DC power (W)	2954	3794	3126	3887	3489	4177
Settling time (s)	0.071	0.060	0.068	0.051	0.062	0.046
Efficiency (%)	67.8	75.5	71.7	77.4	80.0	83.2

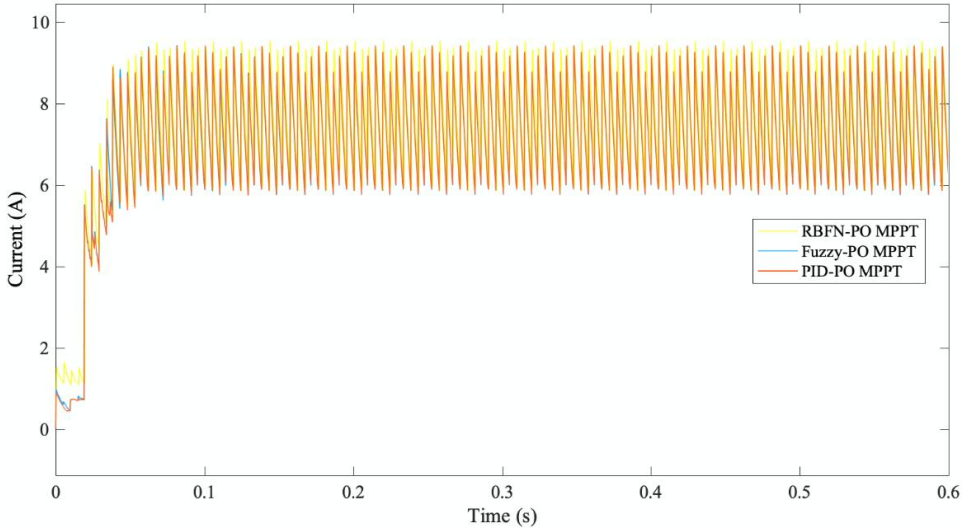

(a)

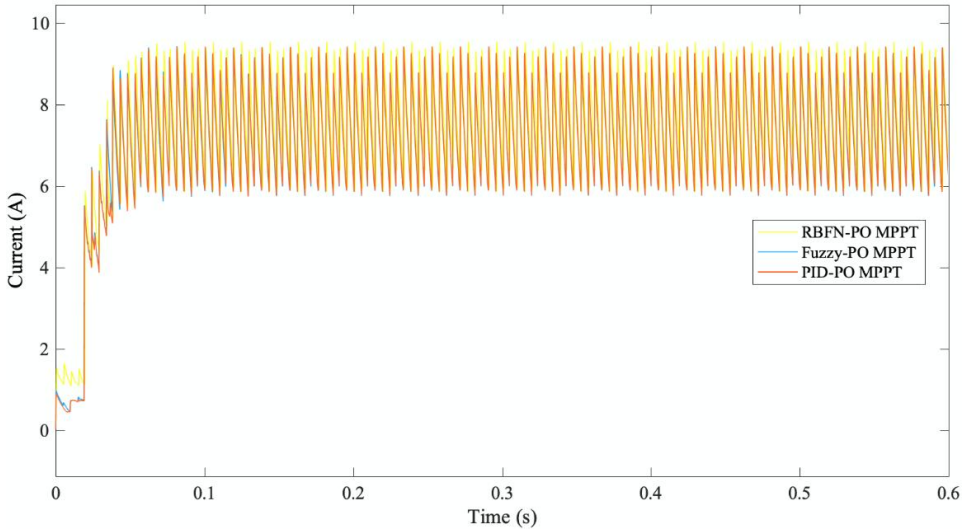

(b)

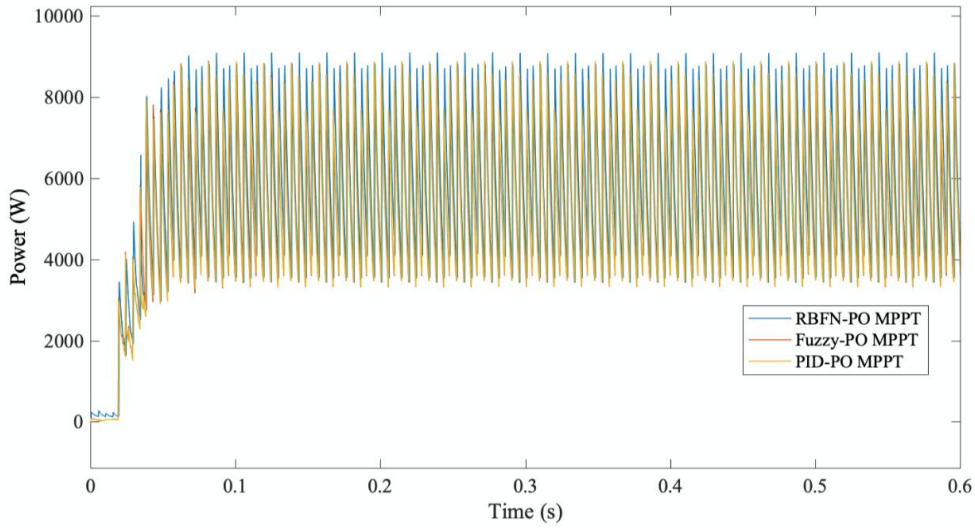

(c)

Fig. 13. Comparison of the output parameters using proposed controllers with M-FLIBC (a) Voltage, (b) current, and (c) Power

4. Conclusions

This article presented an RBFN-P&O based maximum power point controller for the fuel cell system in MATLAB/Simulink platform. The results of the proposed controller in terms of voltage, current, power, settling time, and efficiency are validated with the two more controllers such as PID-P&O and fuzzy-P&O MPPT techniques. From the results, it is evident that the proposed RBFN-P&O controller shows better performance relative to the conventional controllers in terms of maximum power extraction. The major advantage of the proposed MPPT controller is smaller settling time and increased efficiency compared to PID-P&O and fuzzy-P&O MPPT techniques. In future work, we plan to investigate the proposed RBFN-P&O controller for multiple sources like battery-PEMFC- PV systems.

Acknowledgment

The authors declare that there is no competing financial interest or personal relationship that could have appeared to influence the work reported in this paper.

References

[1] Veerendra, Arigela Satya, Mohd Rusllim Mohamed, Pui Ki Leung, and Akeel Abbas Shah. "Hybrid power management for fuel cell/supercapacitor series hybrid electric vehicle." *International Journal of Green Energy* 18, no. 2 (2021): 128-143. https://doi.org/10.1080/15435075.2020.1831511

[2] Bakar, Padilah Abu, Fatin Hana Naning, and Tasiu Zangina. "Electrical Responses of Chitosan-based Biosensor Toward Cadmium Ions Adsorption." *Semarak International Journal of Electronic System Engineering* 1, no. 1 (2024): 26-34. https://doi.org/10.37934/sijese.1.1.2634

[3] Anwer, Abbas Mahmood Oghor, Fuad Alhaj Omar, and Ahmet Afsin Kulaksiz. "Design of a fuzzy logic-based MPPT controller for a PV system employing sensorless control of MRAS-based PMSM." *International Journal of Control, Automation and Systems* 18 (2020): 2788-2797. https://doi.org/10.1007/s12555-019-0512-8

[4] Dzulkarnain, Syarifah Nurfuaduz Zakiah Habib, Mohd Kamal Mohd Nawawi, Rosmaini Kashim, Sharifah Nurul Huda Habib Dzulkarnain, and Syarifah Masyitah Habib Dzulkarnain. "Efficiency Measurement of a Public University: A Slack-Based Data Envelopment Analysis Approach." *Semarak International Journal of Applied Sciences and Engineering Technology* 1, no. 1 (2024): 18-26.

[5] Ma, Raja Noor Farah Azura Raja, Hazwani Abdul Rahim, and Nur Amira Syahirah Azmar. "A Network Model Of Electric Vehicles Charging Station (EVCS) In Malaysia." *Semarak International Journal of Electronic System Engineering* 1, no. 1 (2024): 46-59. https://doi.org/10.37934/sijese.1.1.4659

[6] Bahri, Hamza, and Abdelghani Harrag. "Ingenious golden section search MPPT algorithm for PEM fuel cell power system." *Neural Computing and Applications* 33, no. 14 (2021): 8275-8298. https://doi.org/10.1007/s00521-020-05581-4

[7] Ong, Siew Har, Sai Xin Ni, and Ho Li Vern. "Dimensions Affecting Consumer Acceptance towards Artificial Intelligence (AI) Service in the Food and Beverage Industry in Klang Valley." *Semarak International Journal of Machine Learning* 1, no. 1 (2024): 20-30. https://doi.org/10.37934/sijml.1.1.2030

[8] Zaperi, Nur Husna Amierah Mohd, and Nurul Aini Jaafar. "Solute Dispersion in Casson Blood Flow through a Stenosed Artery with the Effect of Magnetic Field." *Semarak International Journal of Applied Sciences and Engineering Technology* 1, no. 1 (2024): 1-17.

[9] Kamran, Muhammad, Muhammad Mudassar, Muhammad Rayyan Fazal, Muhammad Usman Asghar, Muhammad Bilal, and Rohail Asghar. "Implementation of improved Perturb & Observe MPPT technique with confined search space for standalone photovoltaic system." *Journal of King Saud University-Engineering Sciences* 32, no. 7 (2020): 432-441. https://doi.org/10.1016/j.jksues.2018.04.006

[10] Haron, Nor Hafiza, Nor Hafiza Abd Samad, Anis Juanita Mohd Zainudin, Ramlan Mahmod, and Fatimah Bibi Hamzah. "Automatic Detection System of Open Access Predatory Journals: A Unique Application." *Journal of Advanced Research in Computing and Applications* 33, no. 1 (2023): 1-6. https://doi.org/10.37934/arca.33.1.16

[11] Elgendy, Mohammed A., Bashar Zahawi, and David J. Atkinson. "Assessment of the incremental conductance maximum power point tracking algorithm." *IEEE Transactions on sustainable energy* 4, no. 1 (2012): 108-117. https://doi.org/10.1109/TSTE.2012.2202698

[12] Din, Roshidi, Ahmad Hamid Shakir, Sarmad Hamzah Ali, Alaa Jabbar Qasim Almaliki, Sunariya Utama, and Jabbar Qasim Almaliki. "Exploring Steganographic Techniques for Enhanced Data Protection in Digital Files." *International Journal of Computational Thinking and Data Science* 1, no. 1 (2024): 1-9. https://doi.org/10.37934/CTDS.1.1.19

[13] Mandangan, Arif, and Siti Nurul Hatikah Mohammad. "Colour Image Encryption and Decryption using Arnold's Cat Map and Henon Map." *International Journal of Computational Thinking and Data Science* 1, no. 1 (2024): 41-52. https://doi.org/10.37934/CTDS.1.1.4152

[14] Benyahia, N., H. Denoun, A. Badji, M. Zaouia, T. Rekioua, N. Benamrouche, and D. Rekioua. "MPPT controller for an interleaved boost dc–dc converter used in fuel cell electric vehicles." *International journal of hydrogen energy* 39, no. 27 (2014): 15196-15205. https://doi.org/10.1016/j.ijhydene.2014.03.185

[15] Srinivasan, Suresh, Ramji Tiwari, Murugaperumal Krishnamoorthy, M. Padma Lalitha, and K. Kalyan Raj. "Neural network based MPPT control with reconfigured quadratic boost converter for fuel cell application." *International journal of hydrogen energy* 46, no. 9 (2021): 6709-6719. https://doi.org/10.1016/j.ijhydene.2020.11.121

[16] Aly, Mokhtar, and Hegazy Rezk. "An improved fuzzy logic control-based MPPT method to enhance the performance of PEM fuel cell system." *Neural Computing and Applications* (2022): 1-12.

[17] Aly, Mokhtar, and Hegazy Rezk. "A differential evolution-based optimized fuzzy logic MPPT method for enhancing the maximum power extraction of proton exchange membrane fuel cells." *IEEE Access* 8 (2020): 172219-172232. https://doi.org/10.1109/ACCESS.2020.3025222

[18] Ponnuru, Sudhakiran, R. Ashok Kumar, and NM Jothi Swaroopan. "GWO-based MPPT controller for grid connected Solid oxide fuel cell with high step up DC-DC converter." *Indonesian Journal of Electrical Engineering and Computer Science* 23, no. 3 (2021): 1794-1803. https://doi.org/10.11591/ijeecs.v23.i3.pp1794-1803

[19] Ahmadi, S., Sh Abdi, and M. Kakavand. "Maximum power point tracking of a proton exchange membrane fuel cell system using PSO-PID controller." *International journal of hydrogen energy* 42, no. 32 (2017): 20430-20443. https://doi.org/10.1016/j.ijhydene.2017.06.208

[20] Kumar, Sonu, and Binod Shaw. "Design of off-grid fuel cell by implementing ALO optimized PID-based MPPT controller." In *Soft Computing in Data Analytics: Proceedings of International Conference on SCDA 2018*, pp. 83-93. Springer Singapore, 2019. https://doi.org/10.1007/978-981-13-0514-6_9

[21] Fathy, Ahmed, Mohammad Ali Abdelkareem, A. G. Olabi, and Hegazy Rezk. "A novel strategy based on salp swarm algorithm for extracting the maximum power of proton exchange membrane fuel cell." *International Journal of Hydrogen Energy* 46, no. 8 (2021): 6087-6099. https://doi.org/10.1016/j.ijhydene.2020.02.165

[22] Badoud, Abd Essalam, Saad Mekhilef, and Belkacem Ould Bouamama. "A novel hybrid MPPT controller based on bond graph and fuzzy logic in proton exchange membrane fuel cell system: Experimental validation." *Arabian Journal for Science and Engineering* (2022): 1-20.

[23] Gugulothu, Ramesh, Bhookya Nagu, and Deepak Pullaguram. "A computationally efficient jaya optimization for fuel cell maximum power tracking." *Energy Sources, Part A: Recovery, Utilization, and Environmental Effects* 44, no. 1 (2022): 1541-1565. https://doi.org/10.1080/15567036.2022.2055229

[24] Benyahia, N., H. Denoun, A. Badji, M. Zaouia, T. Rekioua, N. Benamrouche, and D. Rekioua. "MPPT controller for an interleaved boost dc–dc converter used in fuel cell electric vehicles." *International journal of hydrogen energy* 39, no. 27 (2014): 15196-15205. https://doi.org/10.1016/j.ijhydene.2014.03.185

[25] Zhang, Longlong, Dehong Xu, Haijin Li, Guoqiao Shen, and Min Chen. "Three-phase interleaved high step-up boost converter with voltage multiplier for fuel cell power system." In *2015 IEEE Energy Conversion Congress and Exposition (ECCE)*, pp. 4804-4811. IEEE, 2015. https://doi.org/10.1109/ECCE.2015.7310338